Materials and Methods

Analysis of public bulk-RNA-seq data

RNA-seq data from the publicly available databases TARGET (21), including a total of 78 patients in 147 RNA-seq runs, Leucegene (22, 44), including a total of 72 patients in 302 RNA-seq runs, and BEAT-AML2 (23), including a total of 206 patients in 707 RNA-seq runs were downloaded for analysis. AML samples from specific cytogenetic subgroups without mutations in *TET2*, *IDH1* and *IDH2* were selected. **Table S1** summarizes the main clinic-biological features of the analyzed samples and the RNA-seq ID numbers. A total of 119 HIF target genes characterized by hypoxia-dependent transcriptional induction and the presence of functional hypoxia response elements were used to define the hypoxia transcriptomic signature (27) (**Table S2**).

Pre-processing and sample alignments: All samples were processed with the same pipeline and FastQC (79) was used for quality control and confirmation of the sequencing data from the FASTQ files. FASTQ files SRA for TARGET samples were extracted using the SRAToolKit (v 2.9.0) (https://github.com/ncbi/sra-tools).

Gene expression quantification: Illumina paired-end RNA-seq reads were aligned to the Gencode transcriptome release 27 (GRCH38.p10) (80) using Salmon (v0.7.2) (81). Quantification at gene level was performed using pseudo counts from Salmon quantification and transformation to counts per gene using *tximport* library function from Bioconductor (82).

Differential expression analysis: The following AML cytogenetic subgroups were included in the study: NK, inv(16), MLLr, t(8;21), $FLT3^{ITD}$ and $NPM1^{mut}$. The read counts per gene were transformed to log2 counts per million (logCPM) using edgeR (83) and those genes with mean logCPM < 0 were filtered out. Normalization of the data was performed using the TMM method from edgeR package. Differential expression analysis was performed with LIMMA (84) using the function limma.voom adjusted by SVA (85).

Functional enrichment analysis: GSEA was conducted (86) based on the hypoxia transcriptomic signature described above, using the pre-ranked enrichment method, sorting all the genes by $-log_{10}(p-value) \cdot log_2 FC$ obtained from the differential expression analysis.

Primary human cells

Primary AML samples were obtained from accredited biobanks (Finnish Hematology Registry and clinical Biobank (FHRB), Instituto Aragonés de Ciencias de la Salud (IACS) and the VIVO Biobank, supported by Cancer Research UK & Blood Cancer UK (Grant no. CRCPSC-Dec21\100003)) and from collaborating hospitals (Hospital Clinic of Barcelona, Barcelona, Spain; Hospital Princess Maxima, Utrecht, The Netherlands; Hospital Germans Trias i Pujol, Badalona, Spain; Hospital Sant Joan de Déu, Barcelona, Spain; and Hôspital d'enfants Armand Trousseau, Paris, France). Samples were obtained from routine diagnostic procedures after written consent from patients or parents/guardians in case of minors. The study was approved by the Institutional Ethical Review Board of Hospital Clinic of Barcelona (HCB/2018/0020). AML mononuclear cells were frozen until use in liquid nitrogen using fetal bovine serum (FBS) (Sigma) with 10% dimetylsulfoxide (DMSO) (Sigma). The mutational state of AML samples was analyzed on DNA extracted from total cells using the Maxwell RSC Blood DNA Kit (Promega) and a next generation sequencing (NGS) panel of mutations using the Oncomine Myeloid Research Assay (ThermoFisher). **Table S3** lists the main clinico-biological features of the AML samples used in this study.

Healthy CB $CD34^+$ HSPCs were obtained from the Barcelona Blood and Tissue Bank upon Institutional Review Board approval (HCB/2018/0030). $CD34^+$ cells were isolated using anti-human CD34 magnetic beads and the AutoMACS Pro Separator (Miltenyi Biotec) after Ficoll-Hypaque gradient centrifugation (GE Healthcare).

Single-cell RNA sequencing

Sample preparation: Frozen BM AML cells were thawed and stained (30 min at 4ºC) in PBS + 2% FBS with the following antibodies: anti-hCD45-BV510 (HI30), anti-hCD33-BV421 (WM53), anti-hCD34-APC (581) and anti-hCD38-FITC (HIT2) (all from BD Biosciences). Cells were washed with PBS, filtered through a 40-µm strainer and stained with 7AAD (1:100, BD Pharmingen) for 5 min before sorting in FACS Aria-II Fusion cell sorter (BD Bioscience) using a 100-µm nozzle. A minimum of 20,000 cells of each CD34+CD38- (LSC-enriched population) and CD34-CD38+ (LSC-depleted population) sample were collected in PBS + 2% FBS for downstream applications.

Library preparation and sequencing: The cell number and viability of the CD34+CD38- and CD34-CD38+ samples were verified with a TC20™ Automated Cell Counter (BioRad Laboratories) and cells were partitioned into Gel Bead-In-Emulsions using the Chromium Controller system (10X Genomics), with a target recovery of 5,000 total cells of each population. cDNA sequencing libraries were prepared using the Next GEM Single Cell 3' Reagent Kit v3.1 (10X Genomics, PN-1000268). Briefly, after GEM-RT clean up, cDNA was amplified during 12 cycles and cDNA QC and quantification were performed on an Agilent Bioanalyzer High Sensitivity chip (Agilent Technologies). cDNA libraries were indexed by PCR using the PN-220103 Chromiumi7 Sample Index Plate. Size distribution and concentration of 3' cDNA libraries were verified on an Agilent Bioanalyzer High Sensitivity chip (Agilent Technologies). Finally, sequencing of cDNA libraries was done on the Illumina NovaSeq 6000 platform using the following sequencing conditions: 28 bp (Read 1) + 8 bp (i7 index) + 0 bp (i5 index) + 89 bp (Read 2), to obtain approximately 25-30,000 reads per cell.

scRNA-seq data analysis: Reads were aligned to the Hg38 *Homo sapiens* reference genome and quantified through CellRanger Single-Cell Software Suite (v3.1.0). Each sample was analyzed individually prior to data integration. Low-quality cells were filtered out based on mitochondrial RNA percentage, number of unique molecular identifiers (UMIs), and number of different genes (thresholds adjusted separately for each data set). The CD34+CD38- and CD34-CD38+ libraries were merged for each sample before applying usual processing following Seurat tutorials (highly variable genes calculation, log-normalization, scaling and correction by number of UMIs and mitochondrial content). Seurat v4.0.1 was used (87) for R 3.6.1. Principal component analysis (PCA) was performed with a number of principal components ranged between 10 and 20, depending on data set complexity. Dimensionality reduction was performed by applying Uniform Manifold Approximation and Projection (UMAP) algorithm.

The selection of LSC clusters was done independently on each sample. We assigned an LSC6 score for each cell using the six gene signature and weights proposed in Elsayed *et al*, 2020 (35). Due to the sparse nature of the single-cell data, rather than selecting the cells with highest LSC6 score, we elected to cluster the data in an unsupervised manner using the Louvain clustering algorithm with resolution values ranging from 0.5 to 1, and rank the obtained partitions according to their average LSC6 score. Those clusters above

LSC6 decile 9 were determined as the more likely to be enriched on LSCs. If more than one cluster was selected under these criteria, the proportions of *in silico* predictions obtained from Van Galen *et al*, 2019 (37) and Triana *et al*, 2021 (38) were used. The cluster with the highest enrichment of HSC-like predicted cells was finally determined as the most likely to be enriched on LSCs. Cell cycle phases identification was performed based on previously defined markers (88). Scripts and plots generated on each sample are available in Github (https://github.com/JLTrincado/scAML).

In silico prediction of cell types: Some studies have reported phenotypic heterogeneity in human BM. We leveraged these annotated datasets to predict the healthy cell type closest to our leukemic clusters. The annotated healthy BM datasets from Van Galen *et al* (37) was merged and projected onto each sample using FindTransferAnchors and TransferData methods from Seurat (87). Code for reference assembly and projection is available at Github (https://github.com/JLTrincado/scAML). For projecting the data onto healthy BM data from Triana *et al* (38), a workflow based on scmap (89) was used. Sample code for reference atlas projection is available at https://git.embl.de/triana/nrn//tree/master/Projection_ Vignette.

Integration by cytogenetic-molecular subgroup: Seurat canonical correlation analysis (CCA, number of anchors set to 2,000) was applied to correct the patient-specific bias introduced by the pooled transcriptomic information from all sequenced samples (87). Individual clusters identified in each sample to be enriched in LSCs were labeled in the integrated datasets as "LSC^{34}". All the remaining cells not labeled as "LSC^{34}" within the CD34+CD38- population were labeled as "$NonLSC^{34}$". All CD34-CD38+ cells were labeled as "$NonLSC^{38}$".

Pathway scores and pseudotime trajectories: Different gene sets reported in the literature to be associated with LSC-enriched pathways (**Table S2**) were used to biologically inspect each annotated cluster. AddModuleScore from Seurat suite was used to assign a score to each cell for each gene set (87). Resulting values were normalized between 0 and 1. Trajectory analyses were performed with the Monocle package (v2.18.0) (90). The highly variable genes obtained for the integration of the data via Seurat were used for pseudotime ordering. Dimensionality reduction was applied with the DDRTree option.

Analysis of the data from Beneyto-Calabuig et al. cohort: Data from (59) was downloaded from https://doi.org/10.6084/m9.figshare.20291628 and the function AddModuleScore from Seurat was used to compute the average expression of hypoxia related genes. This hypoxia signature, as well as the

normalized expression of HIF1A, were plotted over the myeloid differentiation pseudotime from (59) using a generalized additive model for smoothing. Myeloid differentiation pseudotime was obtained by projecting AML gene expression data to a healthy reference atlas (38) using scmap (89), as described (59).

RNA sequencing bulk analysis

Trimmed and qc-ed reads were mapped onto the human genome (version GRCh38.p14) to compute the counts (Transcripts Per Million; TPM) using Salmon version 1.8.0 (81). Prior to calling differentially expressed genes (DEG) similarity among samples were performed using a PCA analysis on regularized counts using the logarithm transformation as implemented in DESeq2 (91) to identify experimental covariates and batch effects among samples and replicates. DEGs were then identified using DESeq2 (91) at a corrected p-value < 0.001 and a log2 Fold change <= or >= 1.0 . The following comparisons were considered: control vs treatments (AraC, BAY87 and combo); AraC vs combo; BAY87 vs combo; and AraC vs BAY87. Gene ontologies enrichment analyses was based on an F-Fisher test (p-value < 0.001) using the R library topGO (92) with the "weight01" algorithm. Finally, gene signatures were computed using GSVA R package (93).

Cell lines

THP-1, Kasumi-1, ME-1, MV(4;11) and Molm13 cell lines were purchased from the DSMZ German Collection of Microorganisms and Cell Cultures (Braunschweig, Germany). Cells were cultured in RPMI-1640 supplemented with GlutaMAX (Gibco), 10% FBS (20% for ME-1 and Kasumi-1) and penicillin-streptomycin (P/S) (Gibco) at 37ºC with 5% CO_2. MS5 cell line was purchased from the DSMZ German Collection of Microorganisms and Cell Cultures (Braunschweig, Germany). MS5 cells were cultured in αMEM (Gibco) with 10% FBS and penicillin-streptomycin (P/S) (Gibco) at 37ºC with 5% CO_2. MS5 cells were irradiated (50 Gy) and seeded on collagen (StemCell Technologies)-coated plates as monolayers for co-culture with primary AML cells. Cells were passaged every 2-3 days and maintained in an exponential growth phase. All cultures were routinely tested for mycoplasma.

Xenotransplantation

Eight- to twelve-week-old non-obese diabetic (NOD).Cg-*Prkdc*^{scid}*Il2rg*^{tm1Wjl}/SzJ (NSG) mice (The Jackson Laboratory) were bred and housed under pathogen-free conditions. The Animal Care Committee of the Barcelona Biomedical Research Park approved all experimental procedures with mice (HRH-17-0014 and HRH-19-0003). A total of 0.3–1 × 10^6 primary AML cells were intra-BM transplanted into sublethally irradiated (2 Gy) NSG mice (94). AML cells were previously incubated 30 min at 4ºC with OKT3 (BioXCell). Human engraftment was monitored through PB and BM aspirates from week six after transplantation until AML graft levels were ~20% in BM or ~2% in PB. Mice were then homogeneously divided into the following treatment groups (n=5-6/group): (i) AraC (and carrier solution), (ii) BAY 87-2243 (and PBS), (iii) AraC and BAY 87-2243, and (iv) control (PBS and carrier solution). Cytarabine/AraC (50 mg/Kg, Accord) was administered intraperitoneally for 5 days (62, 67). BAY 87-2243 (4 mg/Kg, Selleckchem) was administered for 5 days by oral gavage (66). Mice were sacrificed 48-72 h after treatment completion and PB, BM, spleen and liver were collected to analyze the efficacy of each treatment. White and red blood cell and platelet counts were determined with a hemocytometer (2800VET V-Sight, Menarini Diagnostics). To assess the frequency of AML-LSCs, BM-derived mononuclear cells were collected from primografts (two donor mice with similar human engraftment per treatment group) and were intra-BM transplanted into irradiated (2 Gy) secondary NSG recipients at different doses (n=5/group/cell dose) and were analyzed as above.

Immunophenotyping and cell cycle, apoptosis and CellROX analyses

Immunophenotyping: AML engraftment in mice was monitored by FACS analysis, biweekly in PB and at sacrifice in PB, BM, spleen and liver. PB was collected into EDTA tubes (Sarstedt). Mononuclear cells were stained (30 min at 4ºC) with the following monoclonal antibodies: anti-hHLA-ABC-FITC (G46-2.6), anti-hCD45-APC (HI30), anti-hCD33-PE (WM53), anti-hCD34-PECy7 (8G12) and anti-hCD19-BV421 (HIB19) (all from BD Biosciences). Cells were then lysed and fixed with the BD FACS™ Lysing solution (BD Biosciences). Fluorescence Minus One (FMO) controls were used to set the FACS gates. A FACSCanto™-II flow cytometer and equipped with FACSDiva™ software was used for analysis (BD Biosciences).

Cell cycle analysis: Cells were stained with anti-hCD45-BV510 and anti-hCD33-BV421 (BD Biosciences) for 30 min at 4ºC. After washing, cells were fixed with 0.4% paraformaldehyde (Alfa Aesar) for 30 min at

room temperature (RT), then lysed with 0.2% TritonX (Sigma) for 1 h at 4ºC, washed, stained with anti-Ki67-PE (1:20, BD Biosciences) for 2 h at 4ºC and finally stained with 7AAD (BD Biosciences) for an additional one hour. Cells were analyzed using a FACSCanto™-II flow cytometer and equipped with FACSDiva™ software.

Apoptosis: Cells were washed with Binding Buffer 1X (BD Pharmingen) and stained with anti-hCD33-BV421, anti-hCD45-BV510, anti-hCD34-APC and anti-hCD38-FITC for 30 min at 4ºC. Cells were then washed with Binding Buffer 1X and stained with AnnexinV-PE (BD Biosciences) and 7AAD for 15 min at RT. Cells were analyzed within an hour using a FACSCanto™-II flow cytometer and equipped with FACSDiva™ software.

CellROX: For ROS content analysis, cells were stained with anti-hCD33-BV421, anti-hCD45-BV510, anti-hCD34-PE (581), anti-hCD38-FITC and with CellROX Deep Red Reagent (1:500, ThermoFisher) for 30 min at 37ºC. Cells were washed 3 times with PBS and analyzed using a FACSCanto™-II flow cytometer and equipped with FACSDiva™ software.

Clonogenicity and LTC-IC assays

The clonogenic capacity of leukemic progenitors was evaluated in CFU assays. AML cells (500-50,000 cells/well) were seeded in semisolid methylcellulose media (MethoCult #H4434; StemCell Technologies) according to manufacturer´s instructions. Triplicates of each sample/primograft were seeded. CFU numbers from primograft AML cells were normalized to the total human engraftment of each particular donor mouse. LTC-ICs assays were conducted to evaluate the LSC frequency after *in vitro* treatment with drugs (34, 78). In brief, primary AML BM samples were thawed and seeded on confluent MS5 monolayers on MyeloCult H5100 (StemCell Technologies) supplemented with human IL3 (Miltenyi Biotec), human G-CSF (Amgen) and human TPO (PeproTech) at 20 ng/mL each and 1X P/S (Gibco). Cells were allowed to recover for 48 h and were then treated with the corresponding drugs and maintained for 48 h at 5% O_2 (hypoxic conditions). After drug treatment, AML-MS5 co-cultures were harvested and MS5 cells and T cells were magnetically depleted by AutoMACs (Miltenyi Biotec) using anti-murine Sca1 and anti-human CD3

magnetic beads (Miltenyi Biotec). Recovered cells were counted and different doses (2,000, 1,000, 500 and 250 cells) were seeded each in 15 wells of a 96-well plate pre-coated with MS5 cells in supplemented MyeloCult media and allowed to expand in 20% O_2 (normoxic conditions) with media changes twice weekly. After 5 weeks, wells were score as positive if massive growth of cells were observed in the well (34). LSC dose was determined using ELDA software (95). The identity of the AML cells was confirmed by detection of the molecular alteration by FISH or qPCR.

Fluorescence *in situ* hybridization (FISH)

Cells were resuspended in hypotonic solution (0.075 mM KCl) for 20 min at 37°C and fixed in cold methanol:acetic acid (3:1). Samples were spread onto methanol-cleaned slides and kept at -20°C until processing. Two-color FISH experiments were performed using either XL CBFB, XL t(8;21) (both from MetaSystems) or LSI MLL Break-Apart (Abbott Molecular) probes to detect inv(16), t(8;21) or MLL rearrangements, respectively. FISH was performed following standard procedures (94, 96, 97). Briefly, cells were denatured at 73°C in 70% formamide in 2×SSC for 2 min. Hybridization was carried out by adding 5 µl of the DNA probe mixture to preparations and incubating the slides in a humid chamber at 37°C for 16 h. Post-hybridization washes were performed in 0.4×SSC with 0.3% NP-40 at 73°C followed by 2×SSC with 0.1% NP-40 at RT, for 1 min each. Slides were mounted with DAPI II solution (Abbott Molecular). Analyses were performed using a Nikon Ci-S/Ci-L epifluorescence microscope equipped with specific filters for DAPI, FITC, Cy3 and a dual-band pass filter for FITC and Cy3. A minimum of 200 informative nuclei were analyzed per experiment.

RNA purification and gene expression profiling

RNA was extracted from a pellet of 0.5-1 x 10^6 cells using a Maxwell RSC simply RNA Cells Kit (Promega) on a Maxwell RSC system (Promega). Between 0.2-2 µg of RNA were reverse-transcribed into cDNA using the SuperScript III Reverse Transcriptase (Invitrogen) following manufacturer's instructions. cDNA samples were used as templates for real-time PCR analysis using SYBR Green Mastermix (Invitrogen) on a BIORAD CFXTM Real-Time system (Bio-Rad). Oligonucleotides used are detailed in **Table S4**. Gene expression was normalized with respect to the expression to the housekeeping gene *GUSB*.

RNA for bulk RNA sequencing was extracted using the RNeasy Mini Kit (Quiagen) followed by Illumina sequencing (paired-end 150bp) (Novogene).

Drugs

AraC (Accord) was used at 3 µM *in vitro* and at 50 mg/kg/body weight *in vivo*, administered intraperitoneally daily for 5 days, as described (67). Control animals were treated with the same volume of PBS. BAY 87-2243 (Selleckchem), echinomycin (Sigma) (13) and PX478 (Selleckchem) (98) were used *in vitro* at a final concentration of 10 nM, 500 pM and 10 µM, respectively, previously dissolved in ethanol (Scharlau) (BAY 87-2243) or DMSO (echinomycin and PX478). Control cells were treated with same amount of ethanol/DMSO. For *in vivo* experiments, BAY 87-2243 was dissolved in carrier solution (10% ethanol, 40% solutol HS15 (Sigma), 50% sterile distilled water) and administered orally by gavage (4 mg/kg/body weight) daily for 5 days, as previously described (66). Control animals were treated with the carrier solution.

Statistical analysis

Data are represented as mean ± standard error (SEM). Statistical comparisons between groups were assessed using two-tailed unpaired Student's t-tests, or paired Student's t-tests (when analysing data from same AML samples subjected to different treatments), unless otherwise stated. Data distribution was assumed to normal but this was not formally tested. Variance among groups are assumed as similar but this was not formally tested. All analyses were performed with Prism software, version 8.0 (GraphPad software Inc., San Diego, CA) and $P<0.05$ was considered statistically significant (*$P<0.05$ and **$P<0.01$). No blinding experiments were needed, since values were quantitative comparisons as determined by software and measurements. Sample size was determined based on extensive experience with similar experiments and literature. All samples/mice were analyzed and allocated randomly. Sample exclusion was done only as a result of premature mouse death or if clear errors in pre-processing occurred.

Data and code availability

Newly generated scRNA-seq and bulk RNA-seq data have been deposited on the European Genome-Phenome Archive (EGA) and are accessible through accession no. EGAS00001005980. All analyses and

code used along this study are available at https://github.com/JLTrincado/scAML. All other supporting data/reagents are available upon reasonable request.

Supplemental References

79. Andrews S. FastQC: a quality control tool for high throughput sequence data. Babraham Bioinformatics, Babraham Institute, Cambridge, United Kingdom; 2010.

80. Frankish A, Diekhans M, Ferreira AM, Johnson R, Jungreis I, Loveland J, et al. GENCODE reference annotation for the human and mouse genomes. Nucleic Acids Res. 2019;47(D1):D766-D73.

81. Patro R, Duggal G, Love MI, Irizarry RA, Kingsford C. Salmon provides fast and bias-aware quantification of transcript expression. Nat Methods. 2017;14(4):417-9.

82. Soneson C, Love MI, Robinson MD. Differential analyses for RNA-seq: transcript-level estimates improve gene-level inferences. F1000Res. 2015;4:1521.

83. Robinson MD, McCarthy DJ, Smyth GK. edgeR: a Bioconductor package for differential expression analysis of digital gene expression data. Bioinformatics. 2010;26(1):139-40.

84. Ritchie ME, Phipson B, Wu D, Hu Y, Law CW, Shi W, et al. limma powers differential expression analyses for RNA-sequencing and microarray studies. Nucleic Acids Res. 2015;43(7):e47.

85. Leek JT, Johnson WE, Parker HS, Jaffe AE, Storey JD. The sva package for removing batch effects and other unwanted variation in high-throughput experiments. Bioinformatics. 2012;28(6):882-3.

86. Subramanian A, Tamayo P, Mootha VK, Mukherjee S, Ebert BL, Gillette MA, et al. Gene set enrichment analysis: a knowledge-based approach for interpreting genome-wide expression profiles. Proc Natl Acad Sci U S A. 2005;102(43):15545-50.

87. Stuart T, Butler A, Hoffman P, Hafemeister C, Papalexi E, Mauck WM, 3rd, et al. Comprehensive Integration of Single-Cell Data. Cell. 2019;177(7):1888-902 e21.

88. Kowalczyk MS, Tirosh I, Heckl D, Rao TN, Dixit A, Haas BJ, et al. Single-cell RNA-seq reveals changes in cell cycle and differentiation programs upon aging of hematopoietic stem cells. Genome Res. 2015;25(12):1860-72.

89. Kiselev VY, Yiu A, Hemberg M. scmap: projection of single-cell RNA-seq data across data sets. Nat Methods. 2018;15(5):359-62.

90. Trapnell C, Cacchiarelli D, Grimsby J, Pokharel P, Li S, Morse M, et al. The dynamics and regulators of cell fate decisions are revealed by pseudotemporal ordering of single cells. Nat Biotechnol. 2014;32(4):381-6.

91. Love MI, Huber W, Anders S. Moderated estimation of fold change and dispersion for RNA-seq data with DESeq2. Genome Biol. 2014;15(12):550.

92. Alexa A, Rahnenfuhrer J. topGO: Enrichment analysis for Gene Ontology. R package version 2.28. 0. Cranio. 2016.

93. Hänzelmann S, Castelo R, Guinney J. GSVA: gene set variation analysis for microarray and RNA-seq data. BMC Bioinformatics. 2013;14:7.

94. Diaz de la Guardia R, Velasco-Hernandez T, Gutierrez-Aguera F, Roca-Ho H, Molina O, Nombela-Arrieta C, et al. Engraftment characterization of risk-stratified AML patients in NSGS mice. Blood Adv. 2021.

95. Hu Y, Smyth GK. ELDA: extreme limiting dilution analysis for comparing depleted and enriched populations in stem cell and other assays. J Immunol Methods. 2009;347(1-2):70-8.

96. Molina O, Vinyoles M, Granada I, Roca-Ho H, Gutierrez-Aguera F, Valledor L, et al. Impaired condensin complex and Aurora B kinase underlie mitotic and chromosomal defects in hyperdiploid B-cell ALL. Blood. 2020;136(3):313-27.

97. Molina O, Anton E, Vidal F, Blanco J. Sperm rates of 7q11.23, 15q11q13 and 22q11.2 deletions and duplications: a FISH approach. Hum Genet. 2011;129(1):35-44.

98. Zhang Y, Wang S, Zhang J, Liu C, Li X, Guo W, et al. Elucidating minimal residual disease of paediatric B-cell acute lymphoblastic leukaemia by single-cell analysis. Nat Cell Biol. 2022;24(2):242-52.

Supplemental Figures

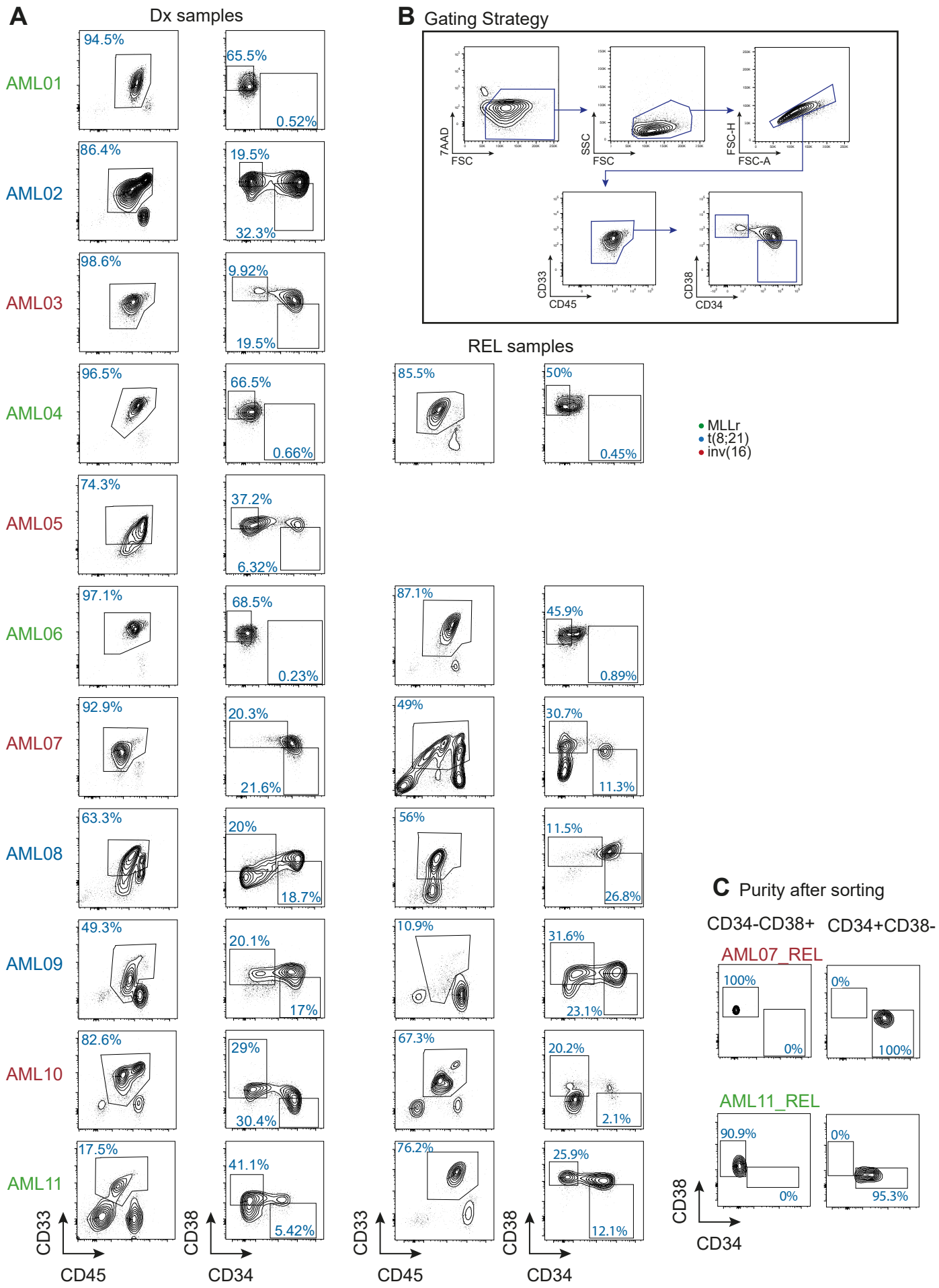
A
Dx samples
AML01
AML02
AML03
AML04
AML05
AML06
AML07
AML08
AML09
AML10
AML11
94.5%
65.5%
0.52%
86.4%
19.5%
32.3%
98.6%
9.92%
19.5%
96.5%
66.5%
0.66%
74.3%
37.2%
6.32%
97.1%
68.5%
0.23%
92.9%
20.3%
21.6%
63.3%
20%
18.7%
49.3%
20.1%
17%
82.6%
29%
30.4%
17.5%
41.1%
5.42%
CD33
CD45
CD38
CD34
B
Gating Strategy
7AAD
FSC
SSC
FSC
FSC-H
FSC-A
CD33
CD45
CD38
CD34
REL samples
85.5%
50%
0.45%
MLLr
t(8;21)
inv(16)
87.1%
45.9%
0.89%
49%
30.7%
11.3%
56%
11.5%
26.8%
10.9%
31.6%
23.1%
67.3%
20.2%
2.1%
76.2%
25.9%
12.1%
CD33
CD45
CD38
CD34
C
Purity after sorting
CD34-CD38+
CD34+CD38-
AML07_REL
100%
0%
0%
100%
AML11_REL
90.9%
0%
0%
95.3%
CD38
CD34

Figure S1. FACS analysis and sorting strategy for each AML sample used in this study (related to Figure 2).

A. FACS plots showing the expression of CD45, CD33, CD34 and CD38 of each Dx and REL AML samples.

B. Stepwise gating strategy used for FACS sorting of the CD34+CD38- and CD34-CD38+ AML subpopulations.

C. FACS plots showing the purity of the sorted populations. Relapsed-AM07 and -AML11 are shown as representative samples.

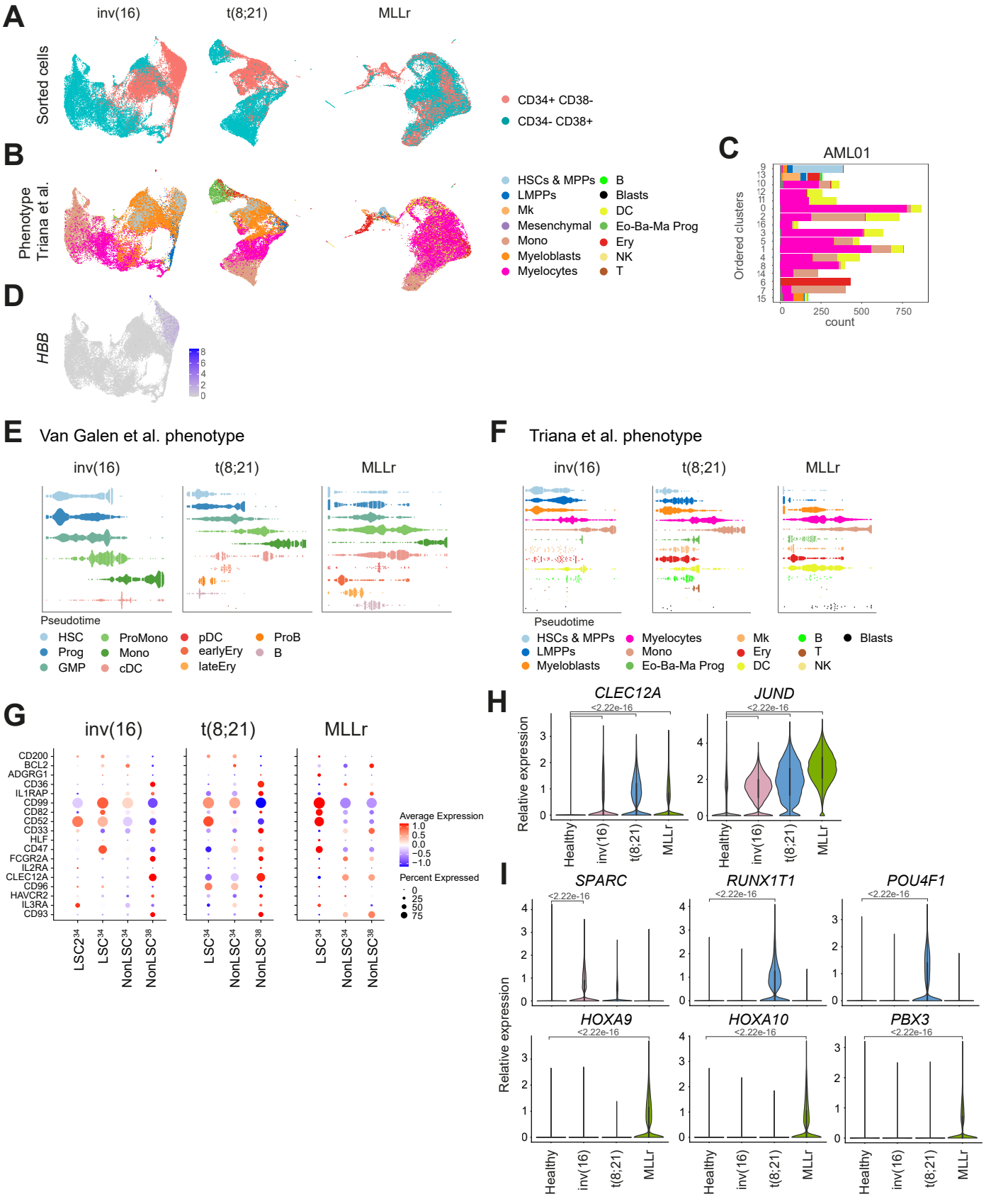
A
inv(16)
t(8;21)
MLLr
Sorted cells
CD34+ CD38-
CD34- CD38+
B
Phenotype Triana et al.
HSCs & MPPs
LMPPs
Mk
Mesenchymal
Mono
Myeloblasts
Myelocytes
B
Blasts
DC
Eo-Ba-Ma Prog
Ery
NK
T
C
AML01
Ordered clusters
count
D
HBB
E
Van Galen et al. phenotype
Pseudotime
HSC
Prog
GMP
ProMono
Mono
cDC
pDC
earlyEry
lateEry
ProB
B
F
Triana et al. phenotype
Pseudotime
HSCs & MPPs
LMPPs
Myeloblasts
Myelocytes
Mono
Eo-Ba-Ma Prog
Mk
Ery
DC
B
T
NK
Blasts
G
CD200
BCL2
ADGRG1
CD36
IL1RAP
CD99
CD82
CD52
CD33
HLF
CD47
FCGR2A
IL2RA
CLEC12A
CD96
HAVCR2
IL3RA
CD93
Average Expression
Percent Expressed
H
CLEC12A
JUND
<2.22e-16
Relative expression
Healthy
inv(16)
t(8;21)
MLLr
I
SPARC
RUNX1T1
POU4F1
HOXA9
HOXA10
PBX3

Figure S2. Single cell transcriptomic characterization of the sequenced AML cells (related to Figure 3).

A. UMAP plots showing from which sorted population (CD34+CD38- or CD34-CD38+) each cell belongs after integrating all samples from each cytogenetic subgroup.

B. UMAP plots showing the predicted phenotype of the cells according to Triana *et at* for all the cells integrated from the different samples in each cytogenetic subgroup.

C. Number of cells from each predicted phenotype according to Triana *et al* included in each cluster of sample AML01.

D. UMAP plot showing the expression of *HBB* in the integrated inv(16) AMLs.

E-F. Trajectory/Pseudotime analysis of the cells included in each of the defined phenotypes according to Van Galen *et al* (**E**) and Triana *et al* (**F**).

G. Comparative relative expression of established stem cell markers in the different defined populations of AML cells.

H. Expression of the AML markers *CLEC12A* and *JUND* in the different AML cytogenetic subgroups compared with healthy BM cells.

I. Expression of the indicated genes in the different AML cytogenetic subgroups compared with healthy BM cells. Overexpression of *SPARC*; *RUNX1T1* and *POU4F1;* and *HOXA9*, *HOXA10* and *PBX3* is well-reported for inv(16), t(8;21) and MLLr AMLs, respectively.

LSC: leukemic stem cell; HSC: hematopoietic stem cell; Prog: progenitor; GMP: granulocyte-macrophage progenitor; ProMono: promonocyte; Mono: monocyte; cDC: conventional dendritic cells; pDC: plasmacytoid dendritic cells; Ery: erythroid progenitor; ProB; B cell progenitor; B: mature B cell; Plasma: plasma cell; T: naïve T cell; CTL: cytotoxic T lymphocyte; NK: natural killer cell; Mk: megakaryocyte ; LMPPs: lymphoid primed multipotent progenitor; MPPs: multipotent progenitor; Eo-Ba-Ma Prog: eosinophil-basophil-mast cell progenitor.

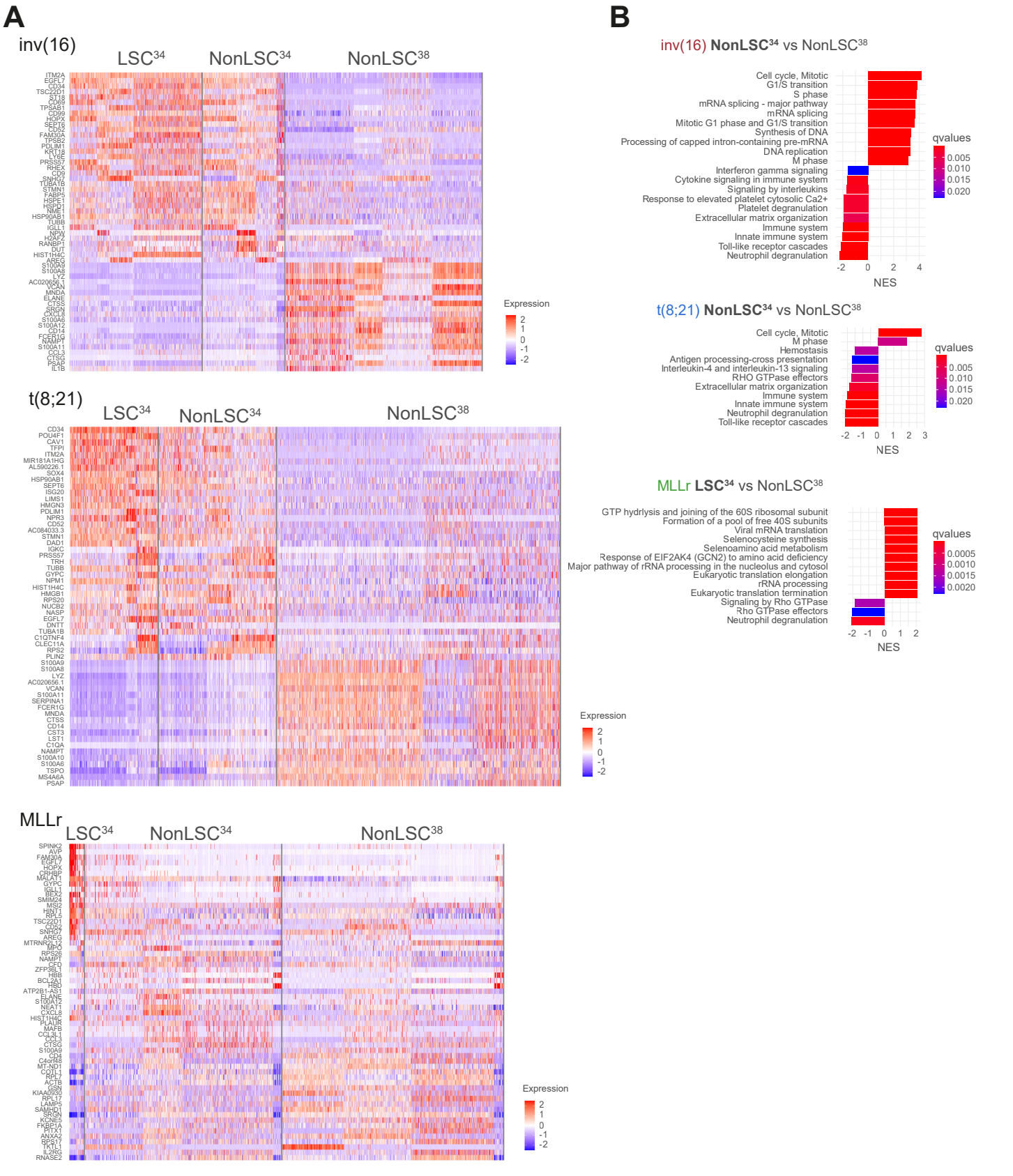
A
inv(16)
LSC34
NonLSC34
NonLSC38
Expression
t(8;21)
MLLr
B
inv(16) NonLSC34 vs NonLSC38
Cell cycle, Mitotic
G1/S transition
S phase
mRNA splicing - major pathway
mRNA splicing
Mitotic G1 phase and G1/S transition
Synthesis of DNA
Processing of capped intron-containing pre-mRNA
DNA replication
M phase
Interferon gamma signaling
Cytokine signaling in immune system
Signaling by interleukins
Response to elevated platelet cytosolic Ca2+
Platelet degranulation
Extracellular matrix organization
Immune system
Innate immune system
Toll-like receptor cascades
Neutrophil degranulation
qvalues
NES
t(8;21) NonLSC34 vs NonLSC38
Cell cycle, Mitotic
M phase
Hemostasis
Antigen processing-cross presentation
Interleukin-4 and interleukin-13 signaling
RHO GTPase effectors
Extracellular matrix organization
Immune system
Innate immune system
Neutrophil degranulation
Toll-like receptor cascades
MLLr LSC34 vs NonLSC38
GTP hydrlysis and joining of the 60S ribosomal subunit
Formation of a pool of free 40S subunits
Viral mRNA translation
Selenocysteine synthesis
Selenoamino acid metabolism
Response of EIF2AK4 (GCN2) to amino acid deficiency
Major pathway of rRNA processing in the nucleolus and cytosol
Eukaryotic translation elongation
rRNA processing
Eukaryotic translation termination
Signaling by Rho GTPase
Rho GTPase effectors
Neutrophil degranulation

Figure S3. Differential gene expression analysis in the defined AML clusters (related to Figure 3).

A. Heatmaps of the DEGs of each of the defined clusters in the 3 cytogenetic groups.

B. GSEA showing the enriched pathways in the different defined clusters of AML cells. For inv(16) and t(8;21) AMLs comparison is shown between $NonLSC^{34}$ and $NonLSC^{38}$ clusters. For MLLr AMLs, comparison is made between LSC^{34} and $NonLSC^{38}$ clusters.

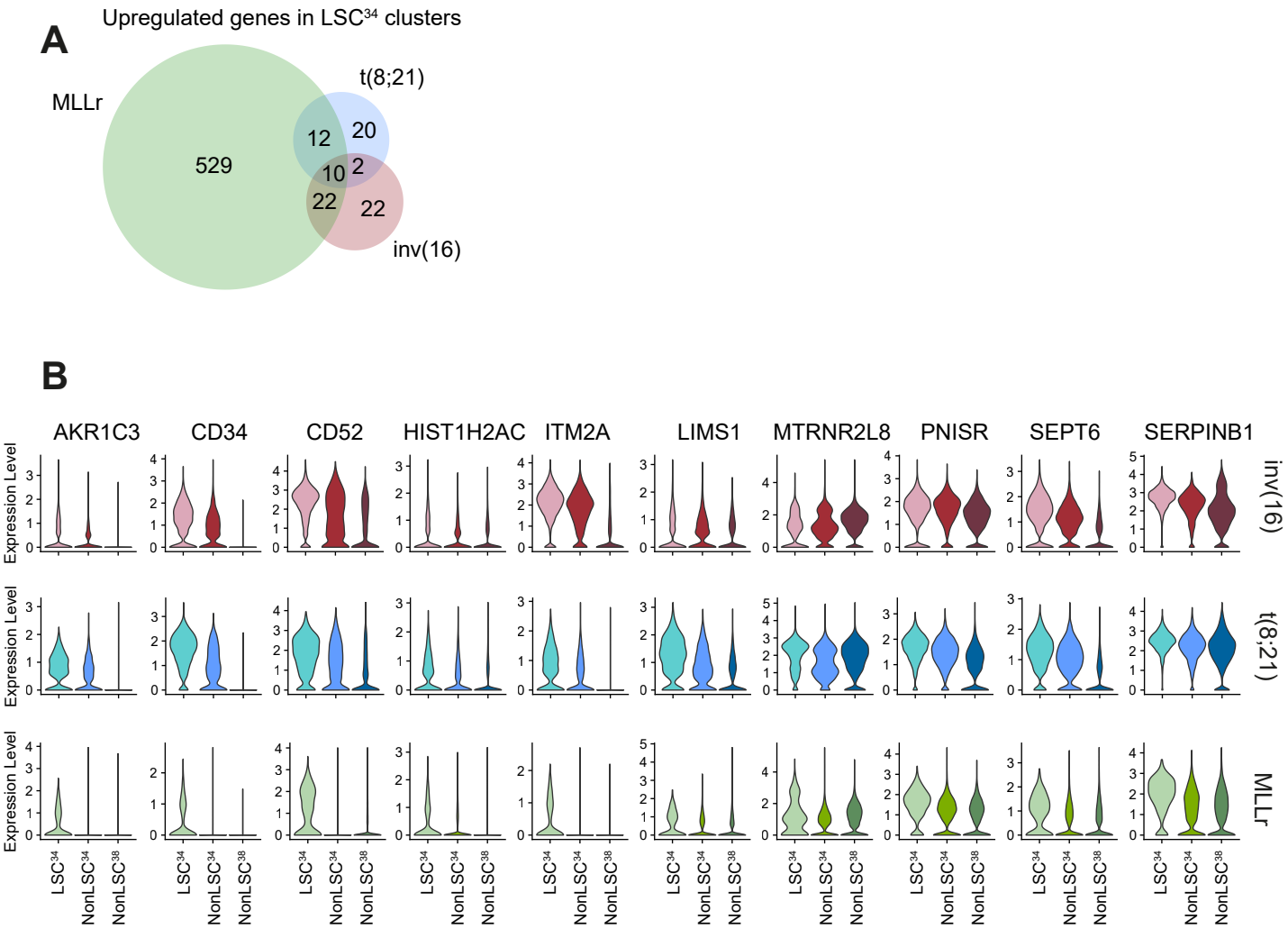
A
Upregulated genes in LSC34 clusters
MLLr
t(8;21)
inv(16)
529
12
20
10
2
22
22
B
AKR1C3
CD34
CD52
HIST1H2AC
ITM2A
LIMS1
MTRNR2L8
PNISR
SEPT6
SERPINB1
Expression Level
inv(16)
t(8;21)
MLLr
LSC34
NonLSC34
NonLSC38

Figure S4. Upregulated genes in the LSC^{34} cluster (related to Figure 3).

A. Venn diagram showing the number of significantly upregulated genes in the LSC^{34} cluster in the different cytogenetic AML subgroups. The number of upregulated genes shared by LSC^{34} cluster of distinct cytogenetic subgroups is also shown.

B. Expression of the 10 genes specifically upregulated in the LSC^{34} clusters shared by the 3 distinct cytogenetic subgroups.

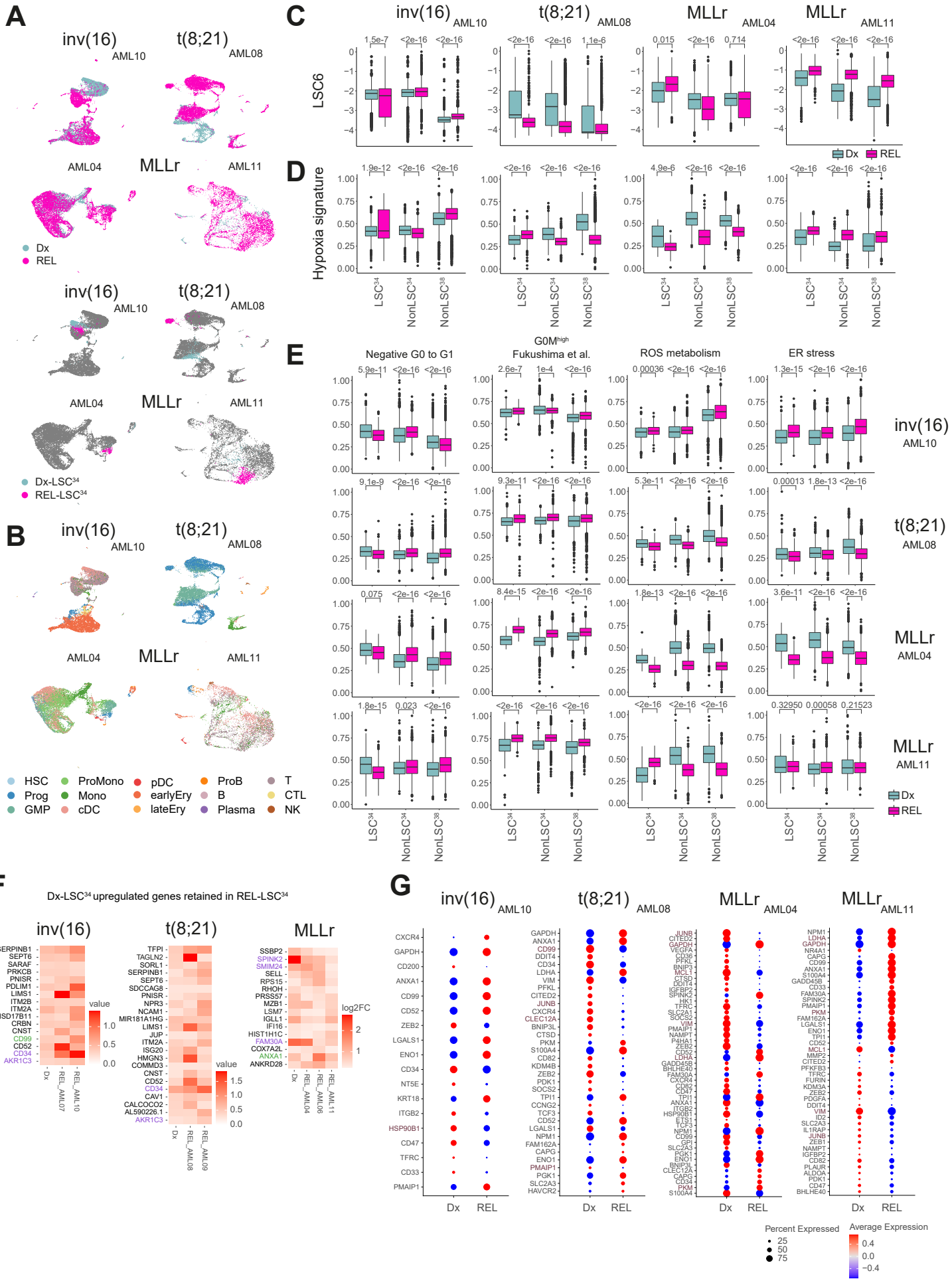
A
inv(16)
AML10
t(8;21)
AML08
AML04
MLLr
AML11
Dx
REL
Dx-LSC34
REL-LSC34
B
HSC
Prog
GMP
ProMono
Mono
cDC
pDC
earlyEry
lateEry
ProB
B
Plasma
T
CTL
NK
C
LSC6
D
Hypoxia signature
LSC34
NonLSC34
NonLSC38
E
G0M high
Negative G0 to G1
Fukushima et al.
ROS metabolism
ER stress
F
Dx-LSC34 upregulated genes retained in REL-LSC34
value
log2FC
G
Percent Expressed
Average Expression

Figure S5. Single cell transcriptomics on paired Dx-REL samples (related to Figure 5).

A. UMAP plots integrating Dx and REL AML cells from the indicated patients (top plots) and showing the identified LSC^{34} cluster at Dx and REL (bottom plots).

B. UMAP plots showing the predicted phenotype according to Van Galen *et al* in the Dx and REL integrated AML cells from the indicated patients.

C-D. LSC6 (**C**) and hypoxia (**D**) signature scores of the defined clusters in Dx and REL AML cells from the indicated patients/cytogenetic subgroups. Nonparametric Wilcoxon test *P* values are shown for each comparison.

E. Analysis of different metabolic pathways related to stemness and hypoxia in the defined clusters in Dx and REL AML cells from the indicated patients/cytogenetic subgroups. Nonparametric Wilcoxon test *P* values are shown for each comparison.

F. Genes commonly overexpressed in the LSC^{34} clusters at both Dx and REL. In purple, genes included in the LSC6 score; in green, hypoxia target genes.

G. Hypoxia target genes differentially expressed between Dx and REL in the indicated paired samples. Genes consistently upregulated or downregulated in all patients from each subgroup are highlighted in brown color.

HSC: hematopoietic stem cell; Prog: progenitor; GMP: granulocyte-macrophage progenitor; ProMono: promonocyte; Mono: monocyte; cDC: conventional dendritic cells; pDC: plasmacytoid dendritic cells; Ery: erytroid progenitor; ProB; B cell progenitor; B: mature B cell; Plasma: plasma cell; T: naïve T cell; CTL: cytotoxic T lymphocyte; NK: natural killer cell; LSC: leukemic stem cell; log2FC: log2 fold change.

A

Sample	Treatment	1/LSC frequency	Range	Fold decrease AraC-combo	*P*-value
AML12	control BAY87 AraC combo	160 210 355 1476	259-98.6 321-136.7 525-240.6 2376-916.3	4.16	*P*<0.0001
AML13	control BAY87 AraC combo	177 110 953 2301	290-107.9 192-63.1 1420-639.5 3873-1367.3	2.41	*P*=0.00856
AML14	AraC combo	4344 21527	11506-1640 153395-3022	4.95	*P*=0.105
AML15	control BAY87 AraC combo	233 536 688 >2194	379-143 947-304 1383-342 >2194	>3.19	*P*=0.00039
AML18	control BAY87 AraC combo	599 806 989 3363	862-416 1164-559 1570-623 5732-1973	3.4	*P*=0.000305
AML19	BAY87 AraC combo	89 910 1361	169-47 1320-628 2027-914	1.49	*P*=0.177

B

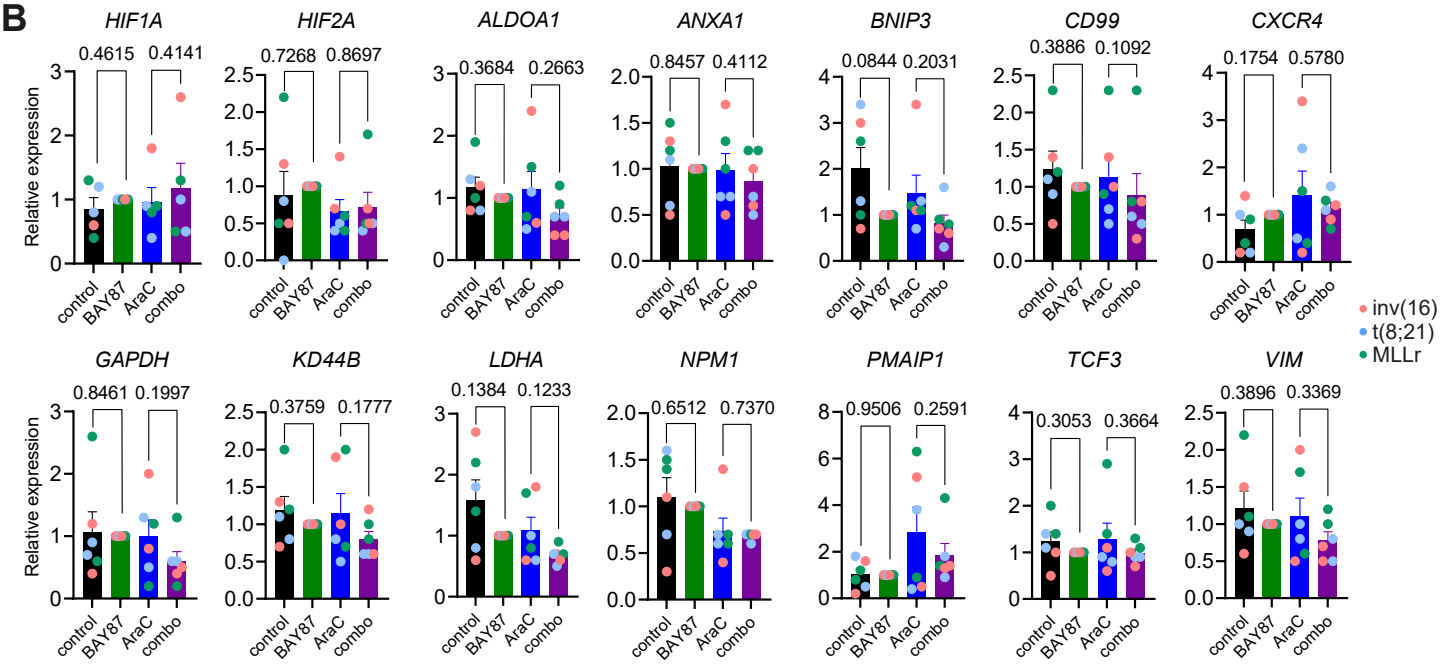

C

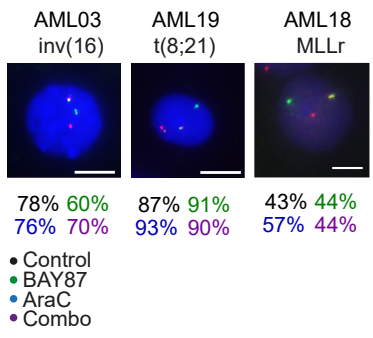

D

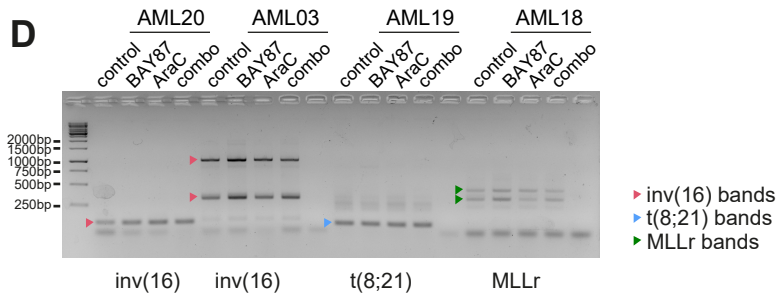

Figure S6. Inhibition of HIF pathway sensitizes AML-LSCs to chemotherapy (related to Figure 6).

A. Detailed estimation of the LSC frequency at the completion of the LTC-IC assay with the ELDA software showing the complete results and differences among the AraC- and combo-treated cultures.

B. Expression of the indicated HIF target genes (identified in the scRNA-seq analysis to be overexpressed in the LSC^{34} cluster) after 48 h of the indicated treatments at 5% O_2 (n=6 samples, AML03, AML16-AML21). Statistical significance was calculated using the paired Student's t test. Expression is normalized respect to the BAY87 samples. Data are shown as mean ± SEM.

C. FISH analysis of the AML cells after 48 h treatment at 5% O_2. Data indicate the percentage of cells harboring the AML-specific rearrangements inv(16), t(8;21) and MLLr. n=200 counted cells. Scale bar = 10µm.

D. qPCR analysis of the treated AML cells, confirming the expression of the gene rearrangement transcript.

Velasco-Hernandez et al. Figure S7

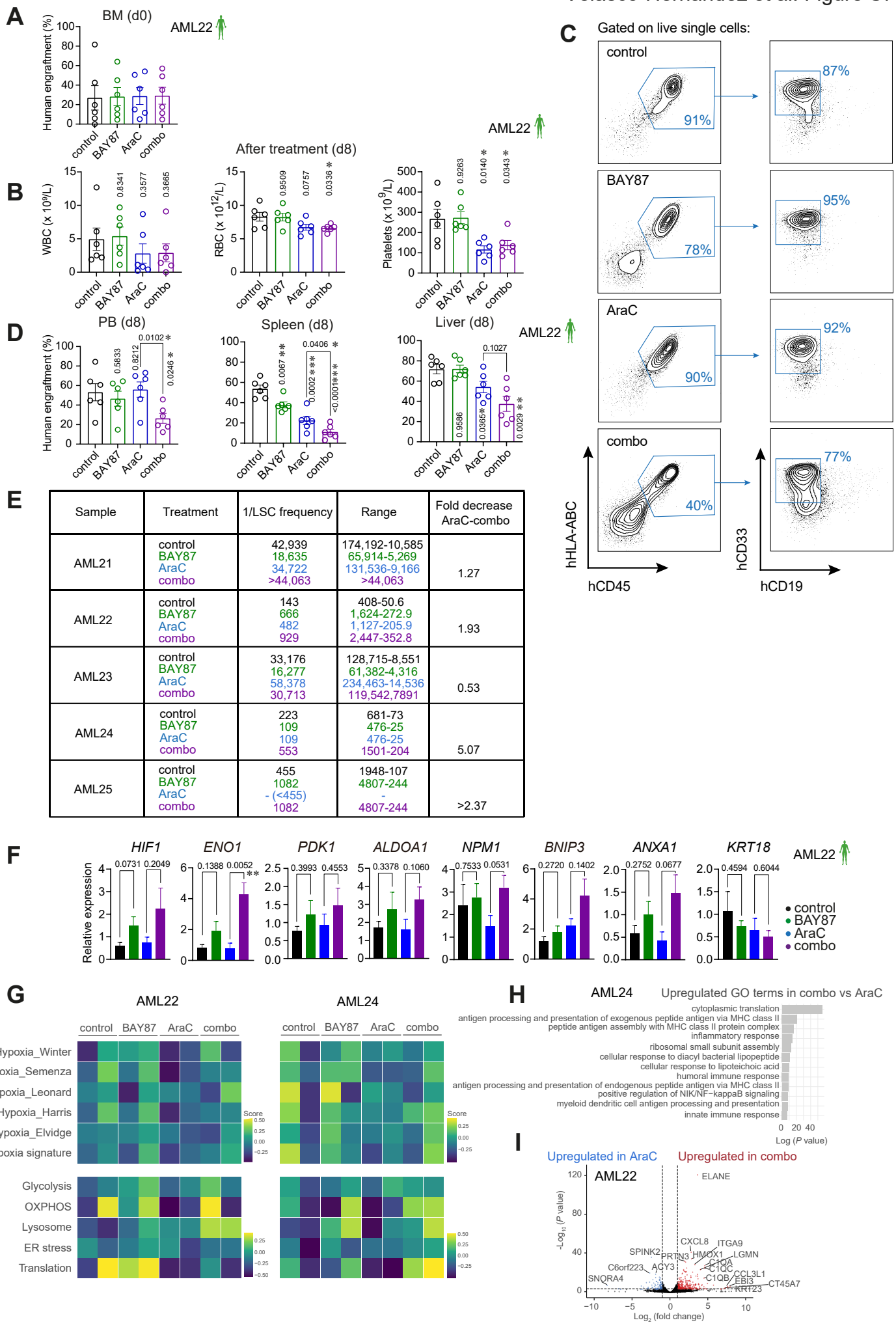

E

Sample	Treatment	1/LSC frequency	Range	Fold decrease AraC-combo
AML21	control BAY87 AraC combo	42,939 18,635 34,722 >44,063	174,192-10,585 65,914-5,269 131,536-9,166 >44,063	1.27
AML22	control BAY87 AraC combo	143 666 482 929	408-50.6 1,624-272.9 1,127-205.9 2,447-352.8	1.93
AML23	control BAY87 AraC combo	33,176 16,277 58,378 30,713	128,715-8,551 61,382-4,316 234,463-14,536 119,542,7891	0.53
AML24	control BAY87 AraC combo	223 109 109 553	681-73 476-25 476-25 1501-204	5.07
AML25	control BAY87 AraC combo	455 1082 - (<455) 1082	1948-107 4807-244 - 4807-244	>2.37

Figure S7. Inhibition of HIF pathway sensitizes AML-LSCs to chemotherapy *in vivo* (related to Figure 7).

A. Human engraftment in BM (hHLA-ABC+ hCD45+ cells) at day 0 (n=6 mice/group). AML22 is shown as a representative sample showing a similar engraftment in all groups before starting the treatment.

B. WBC, RBC and PLT counts in PB of mice treated as indicated (n=6/group). Representative data from AML22. *P*-values of the comparison to control are shown in vertical.

C. Representative FACS plots of BM cells after completion of the treatment**.** Human myeloid (AML) engraftment was identified as hHLA-ABC+ hCD45+ hCD33+ hCD19-.

D. Human myeloid engraftment in the indicated organs after treatment completion (n=6/group). Representative data from AML22. *P*-values of the comparison to control are shown in vertical.

E. Detailed estimation using the ELDA software of the LSC frequency at the completion of the secondary transplants.

F. Expression of the indicated HIF target genes identified in the scRNA-seq analysis as overexpressed in the LSC^{34} cluster, in BM cells of mice treated with the indicated drugs (n=5-6 mice/group). Representative data from AML22.

G. Bulk RNA sequencing analysis was performed from BM cells from treated animals (n=2 mice/group). Heatmap showing the expression of different hypoxia and metabolic signatures.

E. GO terms higher expressed in combo-treated vs AraC-treated samples from AML24.

F. Volcano plot showing the DEGs in AraC and combo-treated samples from AML22.

Data are shown as mean ± SEM. **P* <0.05; ** *P* <0.01; *** *P* <0.001 Student's t test analysis.

Supplemental Tables

Table S1. TARGET, Leucegene and BEAT-AML2 samples analyzed by bulk RNA-seq (related to Figure 1).

Table S2. Gene signatures (related to Figures 1-5).

Table S3. Primary AML samples used in this study (related to Figures 2-7).

Table S4. Primers used for qPCR (related to Figures 6-7).